Uncertainty-Aware Network-Constraint Unit Commitment Problem Considering Mobile Battery Energy Storages and Demand Response Program

Amir Talebi[1], Masoud Agabalaye-Rahvar [1,*] and Kazem Zare [1]

[1] Faculty of electrical and computer engineering, University of Tabriz, Tabriz, Iran
*Corresponding author: m.agabalaye@phd.tabrizu.ac.ir

Manuscript received 18 December, 2025; revised 19 August, 2026; accepted 24 august, 2026. Paper no. JEMT-2512-1586.

The share of renewable energy sources (RESs)-based generation within contemporary power systems has expanded substantially in recent years, driven by environmental concerns and policy incentives to promote clean and sustainable electricity generation. However, the inherently variable and difficult-to-predict behavior of renewable generation, with a particular emphasis on wind-based resources, introduces substantial operational challenges for system operators that require effective flexibility resources. This paper addresses these challenges by formulating a network-constrained unit commitment (NCUC) model that incorporates mobile-based battery energy storage systems (MBESSs) and a price-based demand response program (DRP) as key flexibility resources. A time–space network is employed to optimize the charging, discharging, and transportation schedules of MBESSs. Moreover, a new version of the information gap decision theory (IGDT) method is developed to handle wind power uncertainty more accurately. Unlike the conventional IGDT approach, the proposed method introduces a time-varying uncertainty radius, effectively capturing the dynamic and variable behavior of wind power. The model is formulated as a mixed-integer linear programming (MILP) problem and tested on a six-bus power system integrated with a three-station railway network. Simulation outcomes demonstrate that the proposed framework completely eliminates load shedding and wind power curtailment. Furthermore, compared to the conventional IGDT, the proposed novel method can provide different levels of uncertainty for each interval of the scheduling horizon.

Keywords: *Network-constraint unit commitment, mobile battery energy storage systems, demand response program, uncertainty, time-varying IGDT method*

http://dx.doi.org/10.22109/jemt.2026.567061.1586

1. Introduction

As the Outstanding energy utilization has led to an increase in greenhouse gas (GHG) emissions around the world in recent decades. Therefore, scientists and researchers have been encouraged to deliver uninfected, efficient, and affordable sources of energy. RESs are types of clean and inexpensive energy, which help to decrease emissions [1]. Among these sources, wind energy has been attracting scientists owing to its low generation cost and efficient procedure. Nevertheless, independent system operators have encountered different barriers such as the fluctuating nature of RESs and transmission network congestion. To handle these challenges, energy storage systems (ESSs), typically battery ESSs (BESSs), have been applied as a flexible resource because of non-polluting operation, fast response, and high energy efficiency [2]. In addition, BESSs are designed to deliver security and flexibility for the power systems [3].

Due to limitations of full utilization of RESs capacity in the various buses, the concept of MBESSs [4] has been introduced through the train network, which diminishes network congestion, decreases overall expenditure, and facilitates RESs penetration. MBESSs employ railroads as an additional infrastructure alongside existing network lines, which assist in the transportation of batteries' gathered energy from the power generation areas to the areas with high demand. Another flexible technology is DRPs in power systems, which flatten demand profiles and overcome wind energy variability [5]. Thus, this program will give the opportunity for the clients to control their consumption schema according to the energy prices, which leads to reducing the whole operation cost.

Diverse research works have been implemented on the coordinated operation of BESSs and RESs. Authors in [6] have shown that the incorporation of BESSs into the scheduling and economic optimization of an isolated power system consisting of a significant proportion of wind energy generation has affirmative effect on the power system's economy and RESs' curtailment reduction. SCUC problem for power systems is executed in [7] with a specific ESS named compressed air energy storage and wind energy penetration, in which the conditional-value-at-risk approach has been utilized to handle the stochastic procedure. A stochastic SCUC structure with BESS, wind energy, and line contingency has been proposed in [8].

Ref [9] has outlined the ambiguity of generation and line eventuality via the multi-period stochastic NCUC. A stochastic two-stage SCUC framework for the power systems integrated with plug-in electric vehicles (PEVs) and DRPs has been presented in [10]. The effects of PEVs and DRPs on the power system have been analyzed through a stochastic SCUC programming model [11]. To consider GHG emissions besides economic metrics of power systems, the authors of [12] have proposed a multi-objective probabilistic UC problem considering wind energy uncertainty.

In the aforementioned studies, the analysis of ESSs incorporated in the power system operation has shown that the location of ESSs is fixed, which this action leads to less utilization of available ESSs capacity and RESs generation. Therefore, MBESSs have been attracting by various researchers in recent years. MBESS technology has been combined with SCUC in [13] as a mixed-integer linear programming (MILP), and then the Lagrangian decomposition technique has been employed to alleviate computational time. Authors of [14] have presented a stochastic multi-objective NCUC model integrated with MBESSs to decrease emissions and cost. In order to serve flexibility in the distribution system, ref [15] has presented a two-stage recovery model to manipulate the uncertainties of photovoltaic power and demand by taking into account MBESSs. DRPs are another flexible resource, which results in cost reduction and peak load shaving in the power systems' scheduling. Electrical and thermal consumption demands have been managed via an integrated DRP concept in a large multi-energy consumer in [16] with a robust framework. In another work, as reported in [17], gas consumers' participation in DRP has been carried out within the co-optimization framework to reduce the impact of the gas network on the power grid. Integrating DRP and power-to-gas technologies in the coordinated electricity and gas networks has been presented in [18] through an IGDT-stochastic scheduling model, resulting in lessening environmental pollution and expenditure. In the investigated published research, the deployment of two flexibility resources (MBESS and DRP) has generally been addressed separately. Some studies have considered only fixed ESSs, with or without DRP participation, in power system operation. To address these research gaps, this paper simultaneously implements MBESSs and DRPs within a unified framework. Furthermore, several studies have applied the conventional IGDT method to handle uncertainties. Although IGDT has advantages over stochastic and robust methods (as stated in [19]), it cannot represent a time-varying uncertainty radius. To overcome this limitation, the current paper introduces a new variant of the IGDT method based on the fuzzy membership function (FMF), which provides a time-varying uncertainty radius for wind power modeling. Overall, the proposed work develops an hourly NCUC framework based on the time-varying IGDT method, integrated with MBESS and DRP technologies. This framework enables optimal scheduling of MBESS charging and discharging actions, effectively reducing operation costs, load shedding, and wind power curtailment in the electricity system. Also, the proposed IGDT method provides the system operator with useful insight into dealing with wind uncertainty.

The rest of the paper is as follows. The explanations of the proposed model are provided in Section 2. Section 3 shows the full formulation of the NCUC power system problem with MBESSs and DRP technologies based on the proposed time-varying IGDT approach. Case studies with related discussions are comprehensively indicated in Section 4. Also, the specific discussions about the outstanding findings, strengths and limitations, scope and scalability, and future research directions are provided in Section 5. Section 6 concludes the remarkable points of the paper.

2. Problem Description

This paper introduces an NCUC model for a power system with a high share of wind power. Although wind energy produces clean and affordable electricity, its high penetration can create several operational challenges (such as power line congestion) and may jeopardize the secure operation of the power system. To overcome these limitations, this study deploys MBESSs and DRP as flexibility resources. The transportation and scheduling of MBESSs are optimized using a time–space network (TSN) approach to determine the optimal scheduling plans of the mobile batteries. Moreover, since the conventional IGDT defines a time-independent uncertainty radius for the uncertain parameter, it cannot effectively manage wind power uncertainty throughout the scheduling horizon. Accordingly, the current paper presents a novel time-varying IGDT method that employs the FMF to more effectively capture and manage wind power uncertainty in all scheduling hours. The price-based DRP adopted in this study is based on the load-shifting approach proposed in [16] and [18]. This approach is based on shifting a certain percentage of the load from high-peak to low-peak hours following the electricity price.

The mathematical expressions of the load-shifting approach are given in (25)-(29) and described in detail in Section 3.2. First, note that customer participation is modeled in (25)-(29) by means of the transferable demand variables and shifted-up/down variables, which describe the load-shifting process. In particular, the physical meaning is embedded in the constraints, according to which the amount of shifted-up and shifted-down energy is zero over the relevant scheduling period, thus ensuring that the aggregate customer demand over the scheduling period is constant. In other words, according to the load-shifting approach used in this study, the participation of customers in the DRP is incentivized by means of shifting a part of the load from high-peak hours (associated with a high electricity price) to low-peak hours (associated with a low electricity price). Thus, the mechanism reflects the decision-making process of the price-sensitive customers, who are inclined to shift their consumption from high-price to low-price time slots. In this regard, the response of customers is explicitly considered through the transferable demand variables, while their participation in the DRP is incentivized by the opportunity to reduce their electricity bills by taking advantage of a lower electricity price. Notably, the elasticity of electrical appliances demand is not explicitly considered in the formulation, because it is implicitly considered by means of the amount of load that can be shifted, which is restricted by the technical characteristics of the system. In addition, the incentive mechanism of the DRP under consideration is related to the inherent difference between the incentive-based and price-based DRPs. Specifically, unlike the incentive-based DRP, which explicitly compensates the customers for their participation in the DRP, the price-based DRP implicitly incentivizes the customers to reduce their demand by taking advantage of a lower electricity price during specific time slots.

The practical implications of using a price-based DRP are (1) a necessity for advanced metering infrastructure to communicate prices, (2) a necessity for a reliable communication infrastructure, (3) consumer resistance to frequently changing prices, (4) the need for regulation to protect consumers, and (5) the complexity of introducing DRP and its integration with existing market structures. The proposed model does not explicitly consider all these practical implications. However, we believe that the analysis helps the system operator to identify the maximum potential benefits of implementing any form of DRP and what flexibility such programs offer. We will be able to improve this model in the future and allow for the stochastic nature of participant responses and behaviors.

The proposed NCUC model aims to minimize the whole operational cost of the power system while ensuring secure and reliable operation under wind power uncertainty. In this regard, the time-varying IGDT approach models the uncertain nature of wind generation based on the risk-averse (RA) strategy to provide a robust decision-making strategy against forecast inaccuracy. The model is dependent on a set of technical and operational constraints. In the subsequent section, the NCUC formulation of the power network based on the weighted-IGDT method, integrated with MBESS and DRP technologies, is presented.

3. Problem Formulation

3.1. TSN-Based MBESSs Model

While conventional stationary BESS units offer local flexibility for voltage regulation, reserve provision, and renewable energy integration, their capability to help manage system-wide operational difficulties is inherently restricted by their fixed geographical positioning. In contrast, the MBESSs provide the spatial flexibility, which allows the operators to reposition the storage resources according to real-time system requirements. This inherent mobility provides a number of important advantages over stationary alternatives.

First, MBESS units can help to reduce transmission congestion by delivering stored energy from production-heavy areas to demand-intensive areas without needing any additional transmission infrastructure. This ability is especially useful in networks with a high level of renewable penetration, where it is common that local surpluses will exist next to remote centres of demand. Second, MBESSs can provide location-specific ancillary services, such as peak shaving, ramping support, and congestion management, at different buses on the network at different times of the scheduling horizon. This is an important feature with fixed BESS installations, which are still fixed to a single node. Furthermore, MBESS technology makes the system resilient and able to recover. In situations of network contingencies or network outages, or under extreme weather conditions, mobile storage units can be selectively deployed towards critical facilities for better system survivability. Their reconfigurability also enables them to fill the gap in demand response programs by moving to stations where there is much load-shifting potential and providing support to the grid at the exact time and place that stress is expected. Another important benefit comes in the efficiency of capital utilization. Stationary BESS units can be underutilized when there is no need for charging and discharging at a regular rate under the local conditions. MBESS installations can, however, be distributed over several areas with high levels of operational stress, thereby enhancing the overall economic value of storage assets, while mitigating the risk of stranded capacity. Finally, the integration of MBESS units into a TSN framework offers system operators an opportunity to coordinate transportation and power system decisions at the same time. This holistic approach ensures that the temporal, spatial, and operational constraints are simultaneously optimized, and as a result, system efficiency and operating cost are improved as compared with stationary BESS deployments.

In the proposed framework, the temporal–spatial behavior of each MBESS is represented using a TSN, which provides a structured method for tracking the location, mobility, and operational status of mobile storage units throughout the scheduling horizon. This network is composed of nodes that correspond to specific stations at particular time intervals and arcs that encode the permissible transitions between these nodes. Within this formulation, two distinct categories of arcs are employed. The first category characterizes intervals in which an MBESS remains stationary at a physical station. These arcs enable the unit to engage in charging or discharging activities, as electrical interaction with the grid is feasible only when the MBESS occupies such arcs. The second category captures the transportation of the MBESS between stations, representing the spatial relocation of the unit from one node of the TSN to another [20]. Although both physical and virtual stations appear in the TSN, only the physical stations possess the infrastructure required for power exchange. Virtual stations are included merely to harmonize travel times along extended routes and, therefore, permit only transportation-related arcs.

At each time span s, an MBESS k must be associated with exactly one arc, ensuring a unique operational or transportation status. This requirement is enforced by Equation (1). The continuity of MBESS movement across consecutive time spans is described by constraints (2)–(4). Specifically, if an MBESS k is located at station m at the end of time span s, it must transition in time span $s+1$ onto one of the arcs that emanate from the same station, thereby preserving temporal consistency. These constraints also enforce flow conservation at every node of the TSN, meaning that the number of arcs entering a node is equal to the number leaving it for each MBESS. Equations (3) and (4) separately handle the initial and terminal conditions associated with the first- and final-time spans. The charging and discharging decisions of each MBESS are governed by Equation (5). Charging is activated when $P_{k,m,t} > 0$, thereby drawing power from the grid, whereas discharging occurs when $P_{k,m,t} < 0$, supplying power to the grid. Since electrical exchange is feasible only when an MBESS is stationary, these operations are restricted to the stationary arcs described earlier. The temporal evolution of the stored energy within each unit is captured by the energy balance constraint (6), while the operational limits on storage capacity and power rating are imposed by constraint (7). The terminal energy requirement upon completion of the scheduling period is satisfied through Equation (8).

$$\sum_{mn\in Q} \xi_{k,mn,s} = 1 \qquad ;\forall k, \forall s \tag{1}$$

$$\sum_{mn\in Q_m^+} \xi_{k,mn,s+1} = \sum_{mn\in Q_m^-} \xi_{k,mn,s} \qquad ;\forall k, \forall s = 1,\dots, NS-1 \tag{2}$$

$$\sum_{mn\in Q_m^+} \xi_{k,mn,1} = \xi_{k,m,0} \qquad ;\forall m, \forall k \tag{3}$$

$$\sum_{mn\in Q_m^-} \xi_{k,mn,NS} = \xi_{k,m,NS} \qquad ;\forall m, \forall k \tag{4}$$

$$P_k^{Min}\xi_{k,mm,s} \le P_{k,m,t} \le P_k^{Max}\xi_{k,mm,s} \quad ;\forall m, \forall k, \forall t, \forall s \tag{5}$$

$$E_{k,t} = E_{k,t-1} + \sum_{m} P_{k,m,t} \qquad ;\forall k, \forall t \tag{6}$$

$$E_k^{Min} \le E_{k,t} \le E_k^{Max} \qquad ;\forall k, \forall t \tag{7}$$

$$E_{k,t} = E_{k,NS} \qquad ;\forall k, t = NS \tag{8}$$

Where $k, mn, s,$ and t are the indices of MBESS trains, arcs in TSN from station m to station n, time spans, and hours, respectively; $Q, Q_m^+,$ and Q_m^- are the sets of arcs in TSN in a single time span, arcs in the TSN that originate from station m, and terminate at station m, respectively. The binary variable $\xi_{k,mn,s}$ indicates whether MBESS k traverses arc mn at time span s, while $P_{k,m,t}$ and $E_{k,t}$ denote its charging/ discharging power of MBESSs k at station m and hour t, and stored energy in MBESSs k at hour t, respectively. Parameters $P_k^{Min}, P_k^{Max}, E_k^{Min},$ and E_k^{Max} represent the corresponding lower and upper operational limits of MBESSs k in exchange power and energy capacity, respectively. $\xi_{k,m,0}, \xi_{k,m,NS}$ are the initial and terminal states of MBESSs k at station m.

3.2. Power System Constraints

The power balance constraint for each bus b at hour t is expressed by Eq. (9); the unfolded form of it can be described as follows to illustrate the bus-level structure. An MBESS can be connected to the power system only when it is located on the designated grid-connecting arc, i.e., $\xi_{k,mm,s}=1$. It should be noted that the amount of wind power curtailment and load shedding variables are less than their corresponding values.

$$\sum_{g\in G_b} P_{g,t}+\sum_{w\in W_b}\left(P_{w,t}-WP^{ct}_{w,t}\right)+\sum_{k\in K_b}\sum_{m\in RS}P_{k,m,t} = \sum_{d\in D_b}\left(PD^{AF}_{d,t}-LS_{d,t}\right)+\sum_{l\in \ell_b}P_{l,t} \;;\forall t \tag{9}$$

Where $g,d,l,$ and w are the indices of thermal generation units, electrical demands, transmission lines, and wind power units, respectively. G_b, D_b, ℓ_b, W_b denote the sets of thermal generation units connected to bus b, sets of electrical demands at bus b, sets of transmission lines connected to bus b, and sets of wind power units at bus b, respectively. K_b, RS represent the set of MBESS units located at bus b, and the set of buses with railway stations. $P_{g,t}, PD^{AF}_{d,t}, P_{l,t},$ and $P_{w,t}$ are the produced power of thermal unit g at hour t, consumed electrical demands after applying DRP at hour t, flow on power line l at hour t, and forecasted wind power w at hour t, respectively; $WP^{ct}_{w,t}, LS_{d,t}$ are the wind power spillage w at hour t and load spillage of demand d at hour t.

Thermal generation units' constraints are completely provided as in the subsequent Equations. Electrical power produced by these units is between the minimum and maximum capacities (10). However, producing power between two consecutive hours is limited by ramping up and down according to (11) and (12). Start-up and shut-down indicators of thermal generation units are calculated via the UC model in (13) and (14). The linearized form of the minimum up and down time of these generators is characterized in (15)-(18) and (19)-(22). The detailed expressions for how to model can be found in [21].

$$P^{Min}_g\vartheta_{g,t}\le P_{g,t}\le P^{Max}_g\vartheta_{g,t} \qquad ;\forall g,\forall t \tag{10}$$

$$P_{g,t}-P_{g,t-1}\le(1-Y_{g,t})R^{up}_g+Y_{g,t}P^{Min}_g \qquad ;\forall g,\forall t \tag{11}$$

$$P_{g,t-1}-P_{g,t}\le(1-Z_{g,t})R^{dn}_g+Z_{g,t}P^{Min}_g \qquad ;\forall g,\forall t \tag{12}$$

$$Y_{g,t}-Z_{g,t}=\vartheta_{g,t}-\vartheta_{g,t-1} \qquad ;\forall g,\forall t \tag{13}$$

$$Y_{g,t}+Z_{g,t}\le 1 \qquad ;\forall g,\forall t \tag{14}$$

$$UT_g=Max\left\{0,Min\left[N_T,(T^{ON}_g-X^{ON}_{g,0})\vartheta_{g,0}\right]\right\} \;;\forall g \tag{15}$$

$$\sum_{t=1}^{UT_g}(1-\vartheta_{g,t})=0 \qquad ;\forall g,\forall t \tag{16}$$

$$\sum_{t'=t}^{t+T^{ON}_g-1}\vartheta_{g,t'}\ge T^{ON}_g Y_{g,t} \qquad ;\forall t=UT_g+1,...,N_T-T^{ON}_g+1 \tag{17}$$

$$\sum_{t'=t}^{UT_g}(\vartheta_{g,t'}-Y_{g,t})\ge 0 \qquad ;\forall t=N_T-T^{ON}_g+2,...,NT \tag{18}$$

$$DT_g=Max\left\{0,Min\left[N_T,(T^{oFF}_g-X^{OFF}_{g,0})(1-\vartheta_{g,0})\right]\right\} \;;\forall g \tag{19}$$

$$\sum_{t=1}^{DT_g}\vartheta_{g,t}=0 \qquad ;\forall g,\forall t \tag{20}$$

$$\sum_{t'=t}^{t+T^{OFF}_g-1}1-\vartheta_{g,t'}\ge T^{OFF}_g Z_{g,t} \qquad ;\forall t=DT_g+1,...,N_T-T^{OFF}_g+1 \tag{21}$$

$$\sum_{t'=t}^{DT_g}(1-\vartheta_{g,t'}-Z_{g,t})\ge 0 \qquad ;\forall t=N_T-T^{OFF}_g+2,...,NT \tag{22}$$

Where P^{Min}_g, P^{Max}_g are the minimum and generation capacity of thermal unit g; R^{up}_g, R^{dn}_g denote the maximum allowable upward and downward variations in the output of unit g between consecutive scheduling intervals; $\vartheta_{g,t}$ is the commitment status of thermal generation unit g at hour t. $Y_{g,t}, Z_{g,t}$ are the binary indicators associated with the activation and deactivation processes of unit g at hour t; T^{ON}_g, T^{OFF}_g are the minimum duration requirements for continuous operation and continuous outage of unit g; $X^{ON}_{g,0}, X^{OFF}_{g,0}$ primary on and off conditions of thermal generation unit g.

The real power flow from each transmission line of the power system is calculated via (23) and also restricted by (24). Two types of DRP are known, which means that incentive-based and price-based DRPs could be applied to reduce the electrical demand consumption patterns [22]. In this paper, price-based DRP has been considered such that it can be able to transfer shiftable demand from the high-electricity hours to the low-electricity hours. So, the cost of DRP has not been considered in the objective function. Calculating the net demand after deploying price-based DRP is shown in Eq. (25). In this procedure, how the electrical demand can be transferred to the other periods is denoted by (26), and this transferred demand in the scheduling horizon should be equivalent to zero (27). Finally, the constraints of (28) and (29) represent shifted up and down electrical demand.

$$P_{l,t}=\frac{\delta_{m,t}-\delta'_{m,t}}{X_l} \qquad ;\forall l,\forall t \tag{23}$$

$$-P^{Max}_l\le P_{l,t}\le P^{Max}_l \qquad ;\forall l,\forall t \tag{24}$$

$$PD^{AF}_{d,t}=PD^{BF}_{d,t}+PX_{d,t} \qquad ;\forall d,\forall t \tag{25}$$

$$PX_{d,t}=\left(XS^{up}_{d,t}-XS^{dn}_{d,t}\right)PD^{BF}_{d,t} \qquad ;\forall d,\forall t \tag{26}$$

$$\sum_t PX_{d,t}=0 \qquad ;\forall d \tag{27}$$

$$0\le XS^{up}_{d,t}\le DR^{Max}_{d,t} \qquad ;\forall d,\forall t \tag{28}$$

$$0\le XS^{dn}_{d,t}\le DR^{Max}_{d,t} \qquad ;\forall d,\forall t \tag{29}$$

Where P^{Max}_l is the maximum capacity of the transmission line l; $\delta_{m,t}$ is the voltage angle of the bus m at hour t; X_l is the reactance of the power line l; $PD^{BF}_{d,t}, PX_{d,t}$ are the consumed electrical demands before applying DRP at hour t, and transferable demand d at hour t; $XS^{up}_{d,t}, XS^{dn}_{d,t}$ are the shifts up and down for the electrical demand in the scheduling horizon.

3.3. Objective Function

The whole cost mentioned in the proposed model's objective function (30) consists of three parts. The first part is related to the total fuel cost for generating electric power, startup/ shutdown costs of thermal generation units, and the second part is about the whole MBESS shipment cost. The third part is about wind curtailment and load spillage. As it is obvious, the linearized fuel cost function is utilized instead of the quadratic form in this paper.

$$Min\left\{\begin{array}{l}\sum_{t}\sum_{g\in G_b}\left[FC_g\left(P_{g,t}\right)+SUC_{g,t}+SDC_{g,t}\right]\\+\sum_{k\in K_b}\sum_{mn\in Q}\sum_{s}CT_{k,mn}\xi_{k,mn,s}\\+\sum_{t}\sum_{w\in W_b}CT_{w,t}^{ct}WP_{w,t}^{ct}+\sum_{d\in D_b}\sum_{t}VoLL_{d,t}LS_{d,t}\end{array}\right\} \quad (30)$$

Where $SUC_{g,t}, SDC_{g,t}$, and $CT_{k,mn}$ are the startup and shutdown variable costs of the thermal generation unit g at hour t, and the cost of the transportation of MBESSs k in arc mn, respectively. $CT_{w,t}^{ct}$, $VoLL_{d,t}$ are the cost of wind curtailment w at hour t and the load spillage cost of demand d at hour t.

3.3.1. Discussion on Battery Degradation

Although battery degradation costs are not considered in the proposed NCUC model, in practical applications, it is necessary to take degradation costs into account when conducting long-term economic analysis of the MBESSs.

Battery degradation is mainly caused by the frequent charging and discharging of the battery, thus reducing the battery's capacity. In day-ahead scheduling, the impact of battery degradation can be ignored because the benefits of the optimal operation of the MBESSs in the day-ahead scheduling period cannot compensate for the loss caused by battery degradation in a short period. However, in long-term planning studies, battery degradation costs must be considered in the objective function.

The following extensions can be conducted based on our work to consider battery degradation costs. First, battery degradation costs can be considered as a linear function of the total throughput of the battery because the service life of the battery is related to its capacity. The degradation costs can be expressed by the number of cycles of a battery that is used to determine the replacement interval of the battery. Second, battery degradation can also be related to the depth of discharge. A larger depth of discharge will lead to a faster capacity decline. In addition, calendar aging can be considered in the long-term planning study because the battery capacity will degrade over time even if it is not charged and discharged. These extensions can be easily integrated into our framework for future work.

3.4. Time-Varying IGDT Method for the NCUC Problem

In this section, the uncertainty of wind power is addressed using the proposed time-varying IGDT method. Throughout the scheduling horizon, wind speed (consequently wind power) varies over time, leading to fluctuations in the level of uncertainty. In general, higher wind generation levels are associated with greater forecast uncertainty, and vice versa [23]. The conventional IGDT method cannot effectively capture this dynamic behavior, as it defines a time-independent uncertainty radius for modeling wind uncertainty [24]. In contrast, the proposed IGDT approach introduces a time-varying uncertainty radius, enabling a more accurate and flexible representation of wind power uncertainty across all hours of the scheduling horizon. In this regard, the conventional IGDT method, which is originally a single-objective problem, is transformed into a multi-objective problem under the time-varying IGDT framework, since the time-independent uncertainty radius is decomposed into separate uncertainty radius for each time interval. The fuzzy model is capable of handling the resulting multi-objective problem simultaneously [25]. In the fuzzy model, the objective functions are represented by a membership function, as shown in (31) [26].

$$\mu(\varepsilon_{w,t})=\begin{cases}1 & \varepsilon_{w,t}\geq\varepsilon_{w,t}^{\max}\\ \dfrac{\varepsilon_{w,t}-\varepsilon_{w,t}^{\min}}{\varepsilon_{w,t}^{\max}-\varepsilon_{w,t}^{\min}} & \varepsilon_{w,t}^{\min}\leq\varepsilon_{w,t}\leq\varepsilon_{w,t}^{\max}\\ 0 & \varepsilon_{w,t}\leq\varepsilon_{w,t}^{\min}\end{cases} \quad (31)$$

In the above equation, μ is FMF and $\varepsilon_{w,t}$ is the time-varying uncertainty radius.

After defining FMF, the time-varying IGDT based on the fuzzy model is formulated according to equations (32)-(36). It should be noted that, to ensure robust system operation, the formulation is developed based on an RA strategy [27].

$$max\ \beta \quad (32)$$

$$max\ OF_t \leq (1+\tau).OF_t^B \quad (33)$$

$$(1-\varepsilon_{w,t}).P_{w,t}^{forecasted} \leq P_{w,t} \leq (1+\varepsilon_{w,t}).P_{w,t}^{forecasted} \quad (34)$$

$$\frac{\varepsilon_{w,t}-\varepsilon_{w,t}^{\min}}{\varepsilon_{w,t}^{\max}-\varepsilon_{w,t}^{\min}}\geq\beta \quad (35)$$

$$\text{s.t. (1)-(30)} \quad (36)$$

In the above model, τ is the cost factor and is specified by the operator. OF_t^B denotes the objective function obtained under nominal operating conditions, and its value is achieved by dissolving equations (1)-(30) when $P_{w,t}=P_{w,t}^{forecasted}$. β is the level of satisfaction.

The model described by equations (32)–(36) constitutes a bi-level formulation, thereby yielding a hierarchical optimization structure that lies beyond the direct solution capability of standard solvers. Nevertheless, it could be transformed into a single-level problem based on the RA principle. The RA strategy aims to evaluate the bad impact of uncertain parameters on the objective function [28]. In this regard, a decrease in wind power from its forecasted value represents the worst-case condition that negatively affects the system's operational cost. Accordingly, by applying the RA principle, the bi-level model is restructured into an equivalent single-level optimization problem, as shown in equations (37)–(40).

$$max\ \beta \quad (37)$$

$$OF_t \leq (1+\tau).OF_t^B \quad (38)$$

$$P_{w,t}=(1-\varepsilon_{w,t}).P_{w,t}^{forecasted} \quad (39)$$

$$\text{s.t. (35) and (36).} \quad (40)$$

It should be noted that the values of $\varepsilon_{w,t}^{\min}$ and $\varepsilon_{w,t}^{\max}$ are determined by solving the following model.

$$\varepsilon_{w,t}^{\max} = \max\, \varepsilon_{w,t} \tag{41}$$

$$OF_t \le (1+\tau).OF_t^B \tag{42}$$

$$P_{w,t} = (1-\varepsilon_{w,t}).P_{w,t}^{forecasted} \tag{43}$$

s.t. (1) and (30). (44)

Figure 1 depicts the flowchart of the time-varying IGDT method for the proposed NCUC problem.

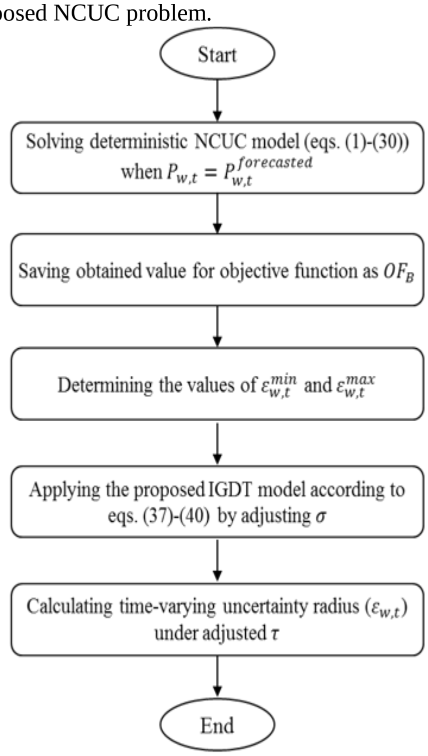

Fig. 1. The considered flowchart of the proposed model.

3.5. Computational Complexity and Scalability Analysis

The proposed NCUC model is formulated as a MILP problem. In this subsection, the complexity of the proposed model is discussed in detail. The number of binary variables of the proposed model is calculated as follows:

$$N_{binary} = T \times (3N_G + N_M \times A_{TSN}/T_s)$$

where T = 24 is the number of scheduling hours, N_G= 3, N_M= 1, A_{TSN} = 312, and T_s = 24. The time-space network comprises 3 physical stations (S1, S2, S3) and 2 virtual stations (S4, S5) to balance the travel time. Specifically, the stationary arcs are 3 stations × 24 hours = 72, and the transportation arcs are 5 connections × 2 directions × 24 hours = 240. Thus, the total number of arcs is 312.

The number of binary variables consists of unit commitment state variables (N_G × T = 72), start-up variables (N_G× T = 72), shut-down variables (N_G× T = 72), and MBESS routing variables (N_M× A_{TSN} = 312). For the test system, the number of binary variables is 528.

The number of constraints comprises power balance constraints (N_B × T = 6 × 24 = 144), thermal unit constraints (ramp rate, min up/down time, and capacity constraints), MBESS routing constraints (flow conservation, energy balance, and capacity constraints), line flow constraints (N_L× T = 7 × 24 = 168) and DRP constraints, which are about 1,847.

As can be seen from Table 4 in Section 4.3, the CPU time of the proposed approach is 39 seconds, which is acceptable for day-ahead scheduling. The MIP solver CPLEX 18.5 with default settings and an MIP gap of 0.01% was used for the calculation. It is worth noting that solving the MILP problem with 528 binary variables and 1,847 constraints takes only 39 seconds, which demonstrates the effectiveness of the proposed method.

4. Simulation Results

The proposed MILP formulation was implemented using the CPLEX 18.5 optimization engine within the GAMS 32 environment and executed on a personal computing platform equipped with an Intel Core i7 processor operating at 2.8 GHz and 8 GB of memory. All required input data, along with four different case studies, are in the following.

4.1. Input Data

The test system is considered as 6 bus power system in this work, which consists of three thermal generation units, three electrical demands, and seven transmission lines, and is shown in Fig. 2. The attributes of all thermal generations, buses, transmission lines, and electrical demands over a 24-h scheduling horizon are extracted from [29]. There are three railway stations $(S1, S2, S3)$ with coordinated MBESS devices. To make the travel time between any two physical stations equal, two virtual stations named as $S4$ and $S5$ are added between $(S1, S2)$ and $(S1, S3)$, respectively. So, the 1 h time span is assumed here. The energy capacity and power rating of the MBESS are set to 120 MWh and 60 MW, respectively, while the charging and discharging efficiencies are both 0.95. The minimum and maximum state of charge (SOC) are 0 MWh and 120 MWh, while the initial SOC is set to 60MWh. Moreover, the hourly demand and the predicted power output of the 100MW wind farm are shown in Fig. 3.

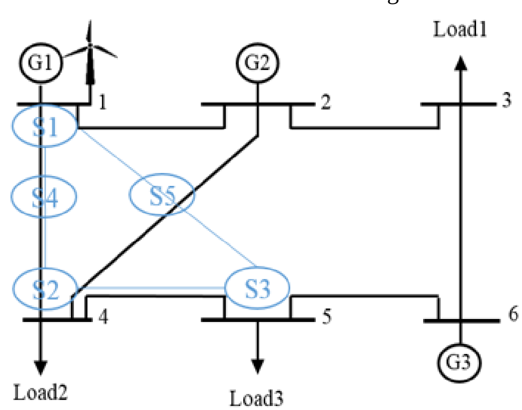

Fig. 2. Power and railway networks.

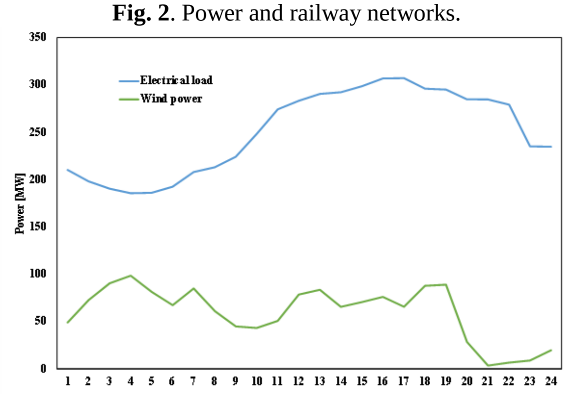

Fig. 3. Forecasted wind power and demand.

4.2. Analysis of different case studies

Four case studies are considered in this paper.

Case 1: Proposed NCUC problem without MBESSs and DRP technologies.

Case 2: Proposed NCUC problem with MBESS devices.

Case 3: Proposed NCUC problem with MBESSs and DRP technologies.

Case 4: Incorporating wind uncertainty in Case 3 through the time-varying IGDT method.

Case 1: In the present Case, the resulting hour-by-hour operational schedule of the NCUC problem indicates that the commitment status of G1 is on all of the hours due to the inexpensive unit; however, the two other units' generations vary according to the electrical demand. This explanation is shown in Fig. 4. Wind curtailment and load shedding amounts are equal to 47.208 MW and 93.168 MW, respectively, and finally, the total operation cost is $190538.3.

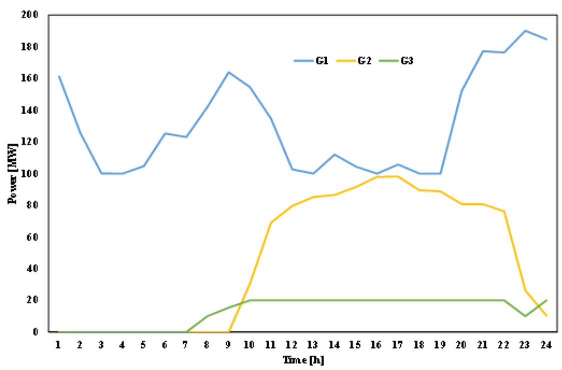

Fig. 4. Hourly scheduling of 3 thermal generation units in Case 1.

Case 2: The role of MBESS is evaluated in this case. The MBESS base station is located at bus 4 (S2). The route plan of the MBESS is presented in Table 1. MBESS begins discharging at bus 4 at hours 1 and 2. It then starts charging at the same bus from hour 3 to hour 6, followed by a brief discharging period at hour 7 and another charging period at hour 8 to reach its maximum energy level. During hours 9 and 10, the MBESS remains idle. Subsequently, it travels to bus 5 (S3) at hour 11. From hour 12 to hour 18, the MBESS continuously discharges power until its stored energy reaches zero. Afterward, it moves from bus 5 (S3) to the virtual bus (S5) and then to bus 1 (S1) during hours 19 and 20, respectively. From hour 21 to hour 22, it charges again before transferring to the virtual bus (S4) and finally returning to bus 4 (S2) in hours 23 and 24. These variations in MBESS energy level are illustrated in Fig. 5.

From the viewpoint of thermal generation, the most economical generating unit (G1) produces more power than in Case 1 during most operating hours, as illustrated in Fig. 6. Moreover, both wind power curtailment and load shedding are reduced compared to Case 1, amounting to 16.15 MW and 21.53 MW, respectively. The total operating cost in this case is $114676.91. It is also noteworthy that, if the ESS were fixed at bus 4, the total cost would increase to $124787.48, confirming the significant positive impact of the MBESS on the NCUC problem.

Table 1. MBESS scheduling route plan in Case 2.

Time span (0-24)	0-10	11	12-18	19
Position of MBESS	S2	S2-S3	S3	S3-S5
Time span (0-24)	20	21-22	23	24
Position of MBESS	S5-S1	S1	S1-S4	S4-S2

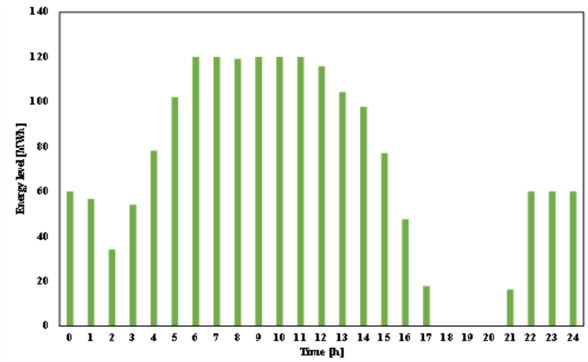

Fig. 5. Variations of the energy level of MBESS in Case 2.

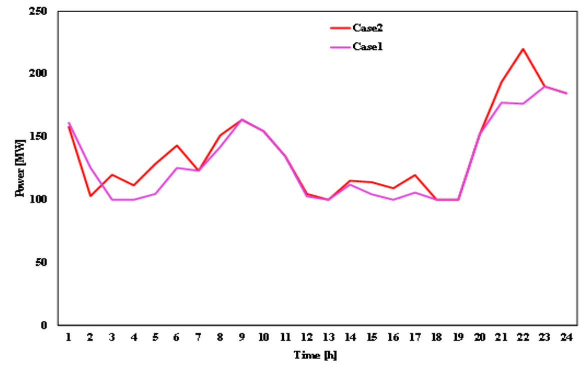

Fig. 6. Comparison of Thermal generation unit G1 in Cases 1 & 2

Case 3: In this case, a price-based DRP is implemented, which influences both the MBESS scheduling route and its charging/discharging patterns. Similar to Case 2, the base station of the MBESS is located at bus 4 (S2). Table 2 reports the route plan of the MBESS in this case. The MBESS begins discharging at bus 4 (S2) from the initial hour to hour 2. It then charges from hour 3 to hour 6 and subsequently discharges again from hour 7 to hour 9. At hour 10, the MBESS transfers to the virtual bus (S4) and then to bus 1 (S1) during hours 10 and 11, respectively. After performing a charging operation at that location, it moves back to the virtual bus (S4) and returns to bus 4 (S2) at hours 13 and 14. Between hours 15 and 19, the MBESS discharges energy until its state of charge reaches zero. It then travels from bus 4 (S2) to the virtual bus (S4) and finally to bus 1 (S1) at hours 20 and 21, respectively. Hour 22 is a charging period for the MBESS. Finally, it returns to its initial base station (bus 4) via the virtual bus (S4) by hour 24. The variations in MBESS energy level are illustrated in Fig. 7.

Figure 8 depicts the electrical demand profiles before and after applying the DRP. As observed, under the proposed DRP**,** a portion of the demand is temporally reallocated away from high-stress intervals toward periods of lower system loading**,** thereby contributing to demand flattening and system cost reduction. A comparison of all three case studies in terms of total operational cost, wind power curtailment, and load shedding is reported in Table 3. The outcomes clearly indicate that, with the implementation of the price-based DRP alongside MBESS scheduling, both load shedding and wind power curtailment are completely eliminated, while the minimum total operating cost is achieved.

Table 2. MBESS scheduling route plan in Case 3.

Time span (0-24)	0-9	10	11	12	13	14
Position of MBESS	S2	S2-S4	S4-S1	S1	S1-S4	S4-S2
Time span (0-24)	15-19	20	21	22	23	24
Position of MBESS	S2	S2- S4	S4-S1	S1	S1- S4	S4-S2

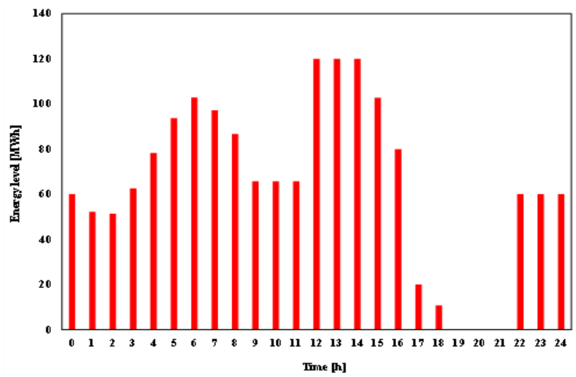

Fig. 7. Variations of the energy level of MBESS in Case 3.

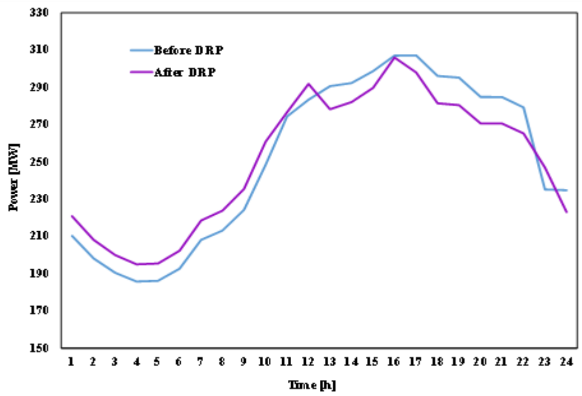

Fig. 8. Comparison of electrical demand before and after applying DRP.

Table 3. Comparison of total cost, wind curtailment, and load shedding in different Case studies.

Case	Total cost ($)	Wind power curtailment (MWh)	Load shedding (MWh)
1	190538.33	47.208	93.168
2	114676.9	16.15	21.53
3	89459	0	0

4.3. Case 4: Uncertainty Analysis

This case incorporates wind power uncertainty into the proposed NCUC model using the time-varying IGDT method. As previously discussed, the conventional IGDT defines a time-independent uncertainty radius for uncertain parameter and, therefore, cannot effectively capture the dynamic and time-varying nature of wind power. In contrast, the proposed IGDT method introduces a time-varying uncertainty radius, which successfully overcomes this limitation of the conventional approach. Fig. 9 presents the comparative results obtained using the time-varying IGDT and conventional IGDT methods. The value of the parameter τ (cost factor) is set to 5%, while the value of OF_B is set to the total cost in Case 3, i.e., $89459. A comparison of the uncertainty radius obtained by the two methods reveals that the proposed IGDT provides time-varying uncertainty levels compared to the conventional IGDT. For instance, at t=4, the uncertainty radius achieved by the time-varying IGDT method is 0.329, whereas under the conventional IGDT method it is 0.229 and remains constant for all scheduling hours. These findings indicate that the proposed IGDT method provides the system operator with a deeper understanding of wind uncertainty and facilitates more effective management of this uncertainty compared to the conventional IGDT approach.

By comparing the uncertainty radius achieved by each method, it is possible to notice that the proposed IGDT has a time-varying uncertainty level while the traditional IGDT has a fixed uncertainty level for all the hours in the studied period. This feature has four significant advantages. Firstly, this method could help the operator to realize which hours have high uncertainty and need extra flexibility to follow the real-time net load. Secondly, this method leads to a reserve scheduling with a superior utilization of flexible resources since the flexibility provided to each hour is related to its uncertainty level. Third, as shown in Fig. 10, the output of G1 can be flexibly adjusted according to the situation. For example, during the hours when the proposed method's uncertainty radius is larger than that of the traditional method (i.e., the proposed method has a larger forecasting uncertainty), the output of G1 is increased to offset the possible shortage of wind power. On the contrary, the output of G1 can be decreased during the hours when the uncertainty of the proposed method is relatively small so as to improve the efficiency. Fourth, it is more reasonable to use the time-varying method since the uncertainty of wind power forecasting tends to increase with the increasing wind power generation.

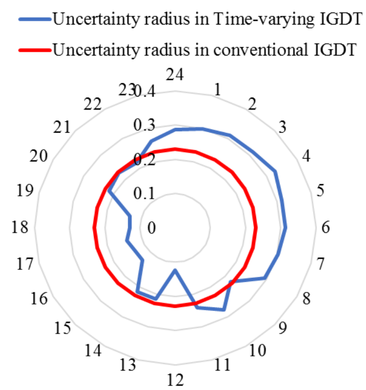

Fig. 9. Results of conventional IGDT and the proposed IGDT.

Thus, while the same total cost is obtained for a specific cost factor (τ), the proposed IGDT method can provide the system operator with better decision-making and resource allocation and, therefore, with more reliable robustness. In addition, Table 4 below compares the proposed and conventional IGDT methods in terms of the required computation time, total cost, and wind utilization. As can be seen, the same total cost is obtained using the two approaches because the cost factor (τ) was selected as 5%. While the computation time needed for the proposed method is higher than that for the conventional method due to the additional calculation of the $\varepsilon_{w,t}^{\min}$ and $\varepsilon_{w,t}^{\max}$ values, it is still acceptable, considering the day-ahead scheduling application. Indeed, 39 seconds is a short time for solving the unit commitment problem formulated as a MILP with binary variables for both the generation and MBESS commitment and routing. Note that the day-ahead scheduling is performed only once a day, and the computation of the solution can be completed within several hours. Table 4 below also shows that the wind utilization in both cases is 100%.

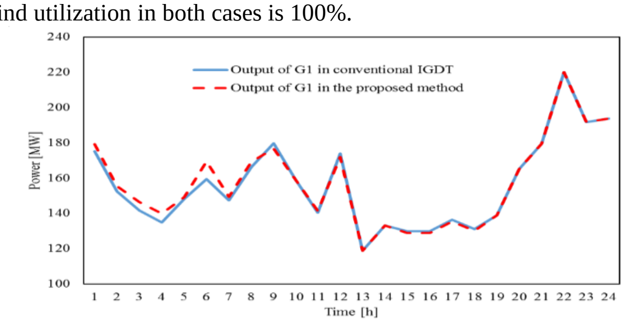

Fig. 10. Output of G1 under conventional and proposed IGDT methods.

Table 4. Comparison of conventional and proposed IGDT methods.

Different system indices / IGDT models	Computation time (s)	Total cost ($)	Wind utilization (%)
Conventional IGDT	11	93931.95	100
Proposed IGDT	39	93931.95	100

4.4. Computational Performance

In this subsection, the computational performance of the proposed MILP formulation is compared. For the same problem, the time to solve the MILP problem using the proposed method is 39 seconds on a personal computing machine with an Intel Core i7 processor at 2.8 GHz and 8 GB of memory, using the CPLEX 18.5 solver with MIP gap set to 0.01%. The number of binary variables and constraints in the problem for the six-bus test system, described in Section 3.5, are 528 and approximately 1847, respectively. This computational time is adequate for the day-ahead scheduling application where typically a few hours are available for computing the solution. The theoretical complexity analysis shows that the number of binary variables is linear in the number of buses and MBESS units, and that the computational time is roughly quadratic in the number of MBESS units. Today's solvers (CPLEX, Gurobi) can work with MILP problems with thousands of binary variables and constraints within a reasonable time frame for day-ahead scheduling. This results in the demonstration of the viability of the proposed solution from computational time perspectives for practical transmission systems.

5. Discussions

5.1. Key Findings

The simulation results in Section 4 demonstrate some remarkable phenomena about the coordination of MBESS and DRP in NCUC with wind power uncertainty.

First of all, comparing Case 2 with Case 1, it can be seen that the use of the MBESS alone (Case 2) significantly reduces wind curtailment and load shedding by 65.8% and 76.9%, respectively. This is because of the spatial flexibility of the coordinated operation of the multi-terminal BESSs. The multi-terminal structure allows the storage system to flexibly transfer electric energy to the node where storage services are needed most, thus eliminating wind curtailment due to line congestion and fully utilizing the renewable power generation. Therefore, the value of spatial flexibility should not be underestimated, especially for the system with a high penetration of renewables.

Second, comparing Case 3 with Case 2, it can be found that the coordinated use of temporal flexibility of DRP and spatial flexibility of MBESS (Case 3) makes it possible to eliminate both wind curtailment and load shedding completely and reduces the total cost by 53.0%, compared with the base case. It can be seen that the temporal flexibility and spatial flexibility can complement each other, and the utilization of both flexibilities can help the system achieve the best operating state.

Finally, it can be seen from the results of Case 4 that the time-varying IGDT method proposed in this paper can effectively solve the problem of the conventional IGDT method, which cannot reflect the characteristics of time-varying uncertainty. As shown in Fig. 9, the uncertainty radius determined by the proposed method varies with the change of time, which is more reasonable compared with the fixed value of the conventional method. Actually, the accuracy of the reserve decision-making depends on the uncertainty radius, and different decisions need to be made for different degrees of uncertainty. In this way, the operator can more rationally arrange the reserve capacity according to the uncertainty of wind power in each period.

5.2. Strengths and Limitations

Strengths:

1. Comprehensive modeling: The proposed framework comprehensively integrates the coordinated planning of MBESS transportation and charging/discharging, DRP participation, and the uncertainty of wind power in a MILP model. The coordinated planning of day-ahead scheduling of the MBESS and the DRP and the consideration of the uncertainty of wind power as a critical source of randomness in the system are the key novelties of this study.
2. Spatial and temporal flexibility: The coordinated scheduling of MBESS transportation and DRP participation yield significant spatial flexibility by exploiting the mobility of the MBESS and substantial temporal flexibility through the DRP.
3. More realistic uncertainty modeling: The proposed time-varying interval method can better capture wind power uncertainty than the conventional interval method.
4. Elimination of wind curtailment and load shedding: The coordinated participation of MBESS and DRP can make wind curtailment and load shedding avoidable (both are zero in our case).

Limitations:

1. Battery degradation: Battery degradation is not considered in the objective function. Although it has a limited impact on the day-ahead scheduling, it should be taken into account when long-term battery degradation is considerable.
2. Customer participation in DRP: Although the participation of industrial/commercial customers in the DRP can be modeled as a parameter in the optimization problem (see Eqs. 25-29), in reality, the participation factor can be different due to various reasons such as comfort, reliability, and technical capability.
3. Computation time: The computational complexity of the MILP formulation may be challenging for large-scale systems. For example, the computation time may increase significantly when the number of buses and/or the number of MBESSs increases. The result in Section 3.5 suggests that the computation time is reasonable for the IEEE 39-bus system. For very large-scale systems, a decomposition-based algorithm may be necessary.
4. The power flow model: The DC power flow is used in this study. It would be valuable to investigate the impact of using the AC power flow model on the performance of the proposed framework. However, the DC power flow model is common in the day-ahead scheduling studies for transmission networks. It is well recognized that the DC power flow model cannot capture the voltage profile and reactive power flow. The AC power flow model is recommended for future work, especially when planning for higher voltage levels.
5. Reliability-oriented metrics: It should be noted that reliability-oriented metrics such as loss-of-load probability (LOLP) and expected energy not served (EENS) are not evaluated in this study, as they are beyond the scope of day-ahead NCUC scheduling and are typically associated with long-term planning or real-time operation studies.

5.3. Validation Scope and Scalability

The method proposed was tested in a test network of 6 buses and 3 stations of a railway, which has been validated. This system size is well suited for the NCUC literature to be validated against the proposed system, and it captures relevant elements of the proposed system such as transmission congestion, spatial mismatch between energy generation and demand, energy storage mobility integration with the railway infrastructure, and uncertainty management. Further validation by applying the proposed approach to larger IEEE benchmark systems, like IEEE RTS-24 or IEEE RTS-39, would further strengthen confidence in the proposed approach; however, the computational workload of these larger systems is still manageable, as will be seen in Section 3.5, and the MILP formulation is easily applicable to practical unit commitment problems. The solution time for the test system with 528 binary variables and 1847 constraints is 39 seconds; thus, the formulation proposed is efficient. The subsequent research will be focused on validating the proposed framework for bigger test systems with real-life datasets to guarantee the utility of the proposed framework in the real world. Moreover, it has to be mentioned that in this research, the primary aim is to develop the day-ahead NCUC scheduling with respect to economic and operational aspects, while loss-of-load probability (LOLP) and expected energy not served (EENS) are not considered in this work, which are normally used in long-term planning or studies for real-time operations.

5.4. Future Research Directions

Apart from the research findings of this work and the proposed solution to the integrated problem of NCUC, there are a few interesting directions for future research.

First, the planning of BESs in the day-ahead unit commitment can be done with consideration of battery degradation and replacement costs. The second future research direction is related to the consideration of customer participation rates in the DRP and their stochastic nature. Third, it would be interesting to consider multiple BESs in the problem to develop coordination strategies for a fleet of BESs. Fourth, future research can consider the integration of other flexible resources, such as plug-in electric vehicles, combined heat and power (CHP) installations, and flexible gas generation. Fifth, future studies may also consider developing control strategies for real-time commitment with a high-resolution unit commitment with the help of the day-ahead scheduling described in this paper. It would be interesting to make the integrated model multi-objective with an objective function that minimizes the emissions of the committed generators while minimizing the operational costs of the system in order to include the environmental concerns of the power system operation, too.

6. Conclusions

This paper proposed an NCUC model for a power system with a high wind power penetration level, considering the flexibility resources of MBESSs and DRP, in which a TSN formulation was applied to optimally schedule the charging, discharging, and transporting of MBESSs. In addition, a novel IGDT method was developed to hedge against wind power uncertainty in a more accurate way by introducing a time-varying uncertainty radius instead of a constant value as used in a conventional IGDT method. The proposed model was formulated as a MILP and was tested on a six-bus power system and a three-station railway system case. This paper showed that compared with the pure wind power system, the utilization of only MBESSs in the power system reduced wind curtailment by 65.8%, from 47.208 MWh to 16.15 MWh, while the reduction of load shedding was 76.9%, from 93.168 MWh to 21.53 MWh. Meanwhile, the coordinated use of both MBESS and DRP technologies in the power system removed both wind curtailment and load shedding to achieve the minimum system operating cost. In addition, the comparative analysis of the conventional and proposed IGDT methods illustrated that the latter can generate a time-varying uncertainty radius while the former keeps the radius constant. As such, the proposed IGDT method allows the system operator to effectively manage time-varying wind power uncertainty.

References

[1] O. Sadeghian and B. Mohammadi-Ivatloo, "Chance-constrained dynamic thermal line rating of power system for enhancing stochastic renewable penetration," *Renewable Energy,* p. 124030, 2025.

[2] C. N. Dimitriadis, E. G. Tsimopoulos, and M. C. Georgiadis, "Optimization-based economic analysis of energy storage technologies in a coupled electricity and natural gas market," *Journal of Energy Storage,* vol. 58, p. 106332, 2023.

[3] M. Kalantar-Neyestanaki and R. Cherkaoui, "Coordinating distributed energy resources and utility-scale battery energy storage system for power flexibility provision under uncertainty," *IEEE Transactions on Sustainable Energy,* vol. 12, no. 4, pp. 1853–1863, 2021.

[4] A. Shoferpour and A. Karimi, "Improving the flexibility of power systems using transportable battery, transmission switching, demand response, and flexible ramping product market in the presence of high wind power," *IET Renewable Power Generation,* vol. 17, no. 6, pp. 1413–1435, 2023.

[5] S. Seyedeh-Barhagh, M. Abapour, B. Mohammadi-Ivatloo, M. Shafie-Khah, and H. Laaksonen, "Optimal scheduling of a microgrid based on renewable resources and demand response program using stochastic and IGDT-based approach," *Journal of Energy Storage,* vol. 86, p. 111306, 2024.

[6] X. Lv, X. Li, and C. Xu, "A robust optimization model for capacity configuration of PV/battery/hydrogen system considering multiple uncertainties," *International Journal of Hydrogen Energy,* vol. 48, no. 21, pp. 7533–7548, 2023.

[7] P. P. Gupta, P. Jain, K. Chand Sharma, and R. Bhakar, "Stochastic scheduling of compressed air energy storage in DC SCUC framework for high wind penetration," *IET Generation, Transmission & Distribution,* vol. 13, no. 13, pp. 2747–2760, 2019.

[8] P. P. Gupta, P. Jain, V. Kalkhambkar, K. C. Sharma, and R. Bhakar, "Stochastic security constrained unit commitment with battery energy storage and wind power integration," *International Transactions on Electrical Energy Systems,* vol. 30, no. 10, p. e12556, 2020.

[9] V. Guerrero-Mestre, Y. Dvorkin, R. Fernández-Blanco, M. A. Ortega-Vazquez, and J. Contreras, "Incorporating energy storage into probabilistic security-constrained unit commitment," *IET Generation, Transmission & Distribution,* vol. 12, no. 18, pp. 4206–4215, 2018.

[10] M. Rahmani, S. H. Hosseinian, and M. Abedi, "Stochastic two-stage reliability-based security constrained unit commitment in smart grid environment," *Sustainable Energy, Grids and Networks,* vol. 22, p. 100348, 2020.

[11] A. G. Trojani, M. S. Moghaddam, and J. M. Baigi, "Stochastic security-constrained unit commitment considering electric vehicles, energy storage systems and flexible loads with renewable energy resources," *Journal of Modern Power Systems and Clean Energy,* 2023.

[12] Y. Zhang, K. Liu, X. Liao, L. Qin, and X. An, "Stochastic dynamic economic emission dispatch with unit commitment problem considering wind power integration," *International Transactions on Electrical Energy Systems,* vol. 28, no. 1, p. e2472, 2018.

[13] Y. Sun, Z. Li, W. Tian, and M. Shahidehpour, "A Lagrangian decomposition approach to energy storage transportation scheduling in power systems," *IEEE Transactions on Power Systems,* vol. 31, no. 6, pp. 4348–4356, 2016.

[14] M. A. Mirzaei *et al.*, "Network-constrained rail transportation and power system scheduling with mobile battery energy storage under a multi-objective two-stage stochastic programming," *International Journal of Energy Research,* vol. 45, no. 13, pp. 18827–18845, 2021.

[15] S. Yao, T. Zhao, H. Zhang, P. Wang, and L. Goel, "Two-stage stochastic scheduling of transportable energy storage systems for resilient distribution systems," in *2018 IEEE International Conference on Probabilistic Methods Applied to Power Systems (PMAPS)*, 2018: IEEE, pp. 1–6.

[16] M. A. Mirzaei, H. Mehrjerdi, and A. M. Saatloo, "Robust Strategic Behavior of a Large Multi-Energy Consumer in Electricity Market Considering Integrated Demand Response," *IEEE Systems Journal,* 2023.

[17] A. Talebi and A. Sadeghi-Yazdankhah, "A Novel Uncertainty Management Method for Economic and Environmental Assessment of Gas-Electricity Networks in the Presence of Flexible Resources," *IET Renewable Power Generation,* vol. 19, no. 1, p. e70113, 2025.

[18] A. Talebi, M. Agabalaye-Rahvar, B. Mohammadi-Ivatloo, K. Zare, and A. Anvari-Moghaddam, "An IGDT-stochastic model for low-carbon economic dispatch of integrated electricity-natural gas systems considering grid-enhancing technologies," *IET Generation, Transmission & Distribution,* 2024.

[19] S. Dorahaki, M. MollahassaniPour, M. Rashidinejad, P. Siano, and M. Shafie-khah, "A flexibility-oriented model for a sustainable local multi-carrier energy community: A hybrid multi-objective probabilistic-IGDT optimization approach," *Applied Energy,* vol. 377, p. 124678, 2025.

[20] K. Zare, A. Akbari-Dibavar, S. Najafi Ravadanegh, and V. Vahidinasab, "Resiliency-oriented scheduling of multi-microgrids in the presence of fuel cell-based mobile storage using hybrid stochastic-robust optimization," *Journal of Energy Management and Technology,* vol. 8, no. 4, pp. 307–320, 2024.

[21] N. Nasiri *et al.*, "A robust bi-level optimization framework for participation of multi-energy service providers in integrated power and natural gas markets," *Applied Energy,* vol. 340, p. 121047, 2023.

[22] M. Tavakoli, M. Khosh Zat, S. Azad, and M. T. Ameli, "Day-Ahead Demand Response in Microgrid Operation Considering Renewable Uncertainty and Network Reconfiguration," *Journal of Energy Management and Technology,* vol. 10, no. 1, pp. 23–34, 2026.

[23] M.-A. Nasr, E. Nasr-Azadani, H. Nafisi, S. H. Hosseinian, and P. Siano, "Assessing the effectiveness of weighted information gap decision theory integrated with energy management systems for isolated microgrids," *IEEE Transactions on Industrial Informatics,* vol. 16, no. 8, pp. 5286–5299, 2019.

[24] Y. Zhang, M. Xiang, and Z. Zheng, "An IGDT-based decision model for industrial users participating in electricity and carbon markets considering differentiated power quality services," *Energy,* vol. 315, p. 134350, 2025.

[25] A. Nikoobakht, J. Aghaei, M. Shafie-Khah, and J. P. Catalão, "Continuous-time co-operation of integrated electricity and natural gas systems with responsive demands under wind power generation uncertainty," *IEEE Transactions on Smart Grid,* vol. 11, no. 4, pp. 3156–3170, 2020.

[26] M. Eslahi, B. Vahidi, and P. Siano, "Novel Time-Varying Risk-Averse and Risk-Seeker Frameworks for Uncertain Wind Energy Generation in Electric Power Systems," *IEEE Access,* 2024.

[27] E. A. Aghdam *et al.*, "A new IGDT-based robust model for day-ahead scheduling of smart power system integrated with compressed air energy storage and dynamic rating of transformers and lines," *Journal of Energy Storage,* vol. 105, p. 114695, 2025.

[28] M. Tostado-Véliz, A. R. Jordehi, S. A. Mansouri, and F. Jurado, "A two-stage IGDT-stochastic model for optimal scheduling of energy communities with intelligent parking lots," *Energy,* vol. 263, p. 126018, 2023.

[29] A. Talebi, A. Mirzapour-Kamanaj, M. Agabalaye-Rahvar, B. Mohammadi-Ivatloo, K. Zare, and A. Anvari-Moghaddam, "Information Gap Decision Theory for Scheduling of Electricity-Gas Systems in the Presence of Demand Response," in *2021 IEEE International Conference on Environment and Electrical Engineering and 2021 IEEE Industrial and Commercial Power Systems Europe (EEEIC/I&CPS Europe)*, 2021: IEEE, pp. 1–6.